

Thermally Induced Errors Modeling and Control for PCMA

Wanli Liu (刘万里)^{1*}, Zhankui Wang (王占奎)², and Xiaoyang Li (李晓阳)²

¹*School of Mechanical and Electrical Engineering, China University of Mining and Technology, Xuzhou 221116, China*

²*Department of Mechanical and Electric Engineering, Henan Institute of Science and Technology, Xinxiang 453003, China*

*Corresponding author: liuwani218@126.com

Received August 20, 2013; accepted October 19, 2013; posted online March 25, 2014

We develop the kinematic model of portable coordinate measuring arm (PCMA) based on the research on its mechanical characteristics and working principle, and present a comprehensive thermally-induced error correction model for PCMA. Based on the model and nominal data provided by a highly accurate coordinate measuring machine, the technique for thermally-induced error compensation of PCMA is presented along with measuring a standard artifact at the corresponding temperature field. Experimental results demonstrate that the deviation of PCMA at different temperatures is controlled in the range of $\pm 10 \mu\text{m}$ using this technique to calibrate the PCMA.

OCIS codes: 120.3940, 120.3930.

doi: 10.3788/COL201412.S11203.

Portable coordinate measuring arm (PCMA) has been successfully introduced into measuring technology. Among large-scale measuring technologies, such as laser tracker, theodolites and photogrammetry, PCMA possesses many advantages, such as light, portability, high speed, and high accuracy, and can be setup readily anywhere in any position. PCMA allows anyone to use it anywhere for the measurement of parts and assemblies directly on the production machinery or surface plate. It is mainly used in the automotive, aerospace, heavy engineering, railway, and energy industries. It is robot-like, driven manually, and allows the user to achieve measurement tasks during maintenance, assembly, quality assurance, inspection, and replication of complex models into three-dimensional (3D) data, or to measure surface of free form and curved pipe lines. The structures of portable measuring arm also allow measurement of work pieces directly in a machine-fastening device. Another application field is in connection with industrial robot calibration^[1,2].

The accuracy level of the PCMA is one of the most important requirements to carry out measurement tasks in the manufacturing industry. To a large extent, PCMA inaccuracy is induced by the propagation of geometric errors and thermally-induced errors. The geometric errors of the PCMA due to manufacturing imperfections, whereas thermally-induced errors are due to thermal distortion and expansions of PCMA components due to internal and external temperature change. Previous research on PCMA calibration focused mainly on PCMA geometric errors, as summarized by SANTOLARIA^[3] and KOVAC^[4]. However, the thermally-induced errors also play a significant role, especially when high accuracy is desired.

Real-time thermally-induced error compensation techniques have been successfully applied to coordinate

measurement machine (CMM) and a series of machining systems. Unlike CMM, the thermally-induced behavior of PCMA has not been extensively investigated yet. The main reason is probably due to the fact that the accuracy requirement for most of the PCMA applications is not as high as that for machine tools. It has been observed that temperature variation has a profound effect on PCMA performance. Nevertheless, the influence of thermal changes on the accuracy of PCMA is one of their main sources of error. Usually, the effects of this problem are minimized by using low thermal-expansion materials in the arm design or by implementing an empirical error correction model based on the outputs of several temperature sensors placed inside the arm. These models, inherited from temperature correction models for arms, are based on the empirical arm positioning error characterization of several temperatures inside its measuring range and posterior corrections implemented using an average error approximation. Considering this approximation as a correction valid for all the temperature ranges violates the PCMA calibration conditions, which are defined by a kinematic parameter identification procedure at a reference temperature. This implies that by applying these models, the PCMA works outside of calibration conditions and does not meet the nominal accuracy values obtained from the identification procedure^[5,6].

Therefore, at present, there is a critical need to overcome disadvantages in existing techniques and to compensate the thermally-induced errors of PCMA in the workspaces. This paper develops a novel comprehensive thermally-induced error correction model for PCMA.

A general methodology is developed to calibrate these errors simultaneously. Based on these models and the nominal data provided by a high-accuracy CMM, a new technique for thermally-induced error compensation

of PCMA has been presented along with measuring a standard artifact placed in several positions at the corresponding temperature field. Experimental results demonstrate that the measuring accuracy of PCMA has been sharply improved after the compensation using this technique to calibrate the PCMA.

As shown in Fig. 1, the PCMA mainly includes six joints (1–6), probe 7, and mount 8. The measuring principle of the PCMA is that it works like human arm, but with more precision and greater flexibility. Measurements can be obtained from a variety of locations with the help of various mounting options, e.g., magnetic or vacuum mounts. When the probe of PCMA is placed on the measurement position, each joint relative rotational $\theta_i (i = 1, 2, \dots, 6)$ obtained by highly accurate shaft encoders allows PCMA to compute the position of the probe at any time in 3D space.

The static calibration of a PCMA establishes a parametric model^[7,8] of its kinematic behavior in order to determine, numerically, the relationship between the joint variables and the probe position for any arm posture. A direct kinematic model takes the form

$$y = f(\theta_i, q), \quad (1)$$

where, $i = 1, \dots, n$ for an arm with n rotating joints. This model calculates the position and orientation of the PCMA probe y , according to the value of the joint variable θ_i and the equations of the model defined in f , which depends on the parameter vector θ . This parameter vector contains the geometric parameters of the model, which must be optimized in order to obtain the lowest possible measurement error. Depending on the chosen kinematic model, the equations are obtained as f changes, along with the number of geometric parameters necessary to be included in q . The D–H basic model uses four parameters (d_i, a_i, θ_i and α_i) to model the transformation of coordinates between successive reference systems. The homogeneous transformation matrix between frame i and $i - 1$ [Eq. (2)] depends on those four parameters^[9,10].

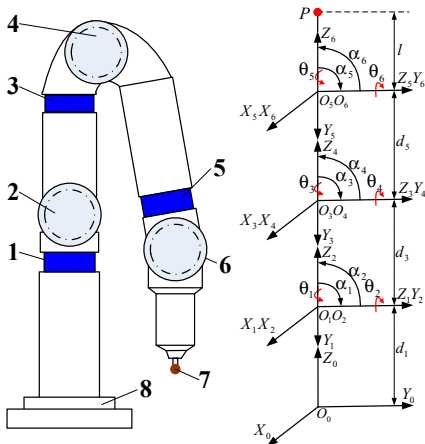


Fig. 1. Kinematic model of PCMA.

$${}^{i-1}A_i = T_{z,d} T_{z,\theta} T_{z,a} T_{z,\alpha}$$

$$= \begin{pmatrix} \cos \theta_i & -\cos \alpha_i \sin \theta_i & \sin \alpha_i \sin \theta_i & a_i \cos \theta_i \\ \sin \theta_i & \cos \alpha_i \cos \theta_i & -\sin \alpha_i \cos \theta_i & a_i \sin \theta_i \\ 0 & \sin \alpha_i & \cos \alpha_i & d_i \\ 0 & 0 & 0 & 1 \end{pmatrix}. \quad (2)$$

During the measurement, small errors in the end-effector position could not be modeled by small errors in the D–H link parameters in case of two consecutive joints of PCMA. This causes numeric instability during the identification process. In order to avoid the singularity problem, a small rotation of β about the axis y , $Rot(y, \beta)$ is added. As for the PCMA consecutive joints, the homogenous transformation A_i becomes

$$A_i = \begin{pmatrix} c\theta_i c\beta_i - s\theta_i s\alpha_i s\beta_i & -c\alpha_i s\theta_i & c\theta_i s\beta_i - s\theta_i s\alpha_i c\beta_i & a_i c\theta_i \\ s\theta_i c\beta_i + c\theta_i s\alpha_i s\beta_i & c\alpha_i c\theta_i & s\theta_i s\beta_i - c\theta_i s\alpha_i c\beta_i & a_i s\theta_i \\ -c\alpha_i s\beta_i & s\alpha_i & c\alpha_i c\beta_i & d_i \\ 0 & 0 & 0 & 1 \end{pmatrix}, \quad (3)$$

where, s and c represent \sin and \cos , respectively.

By calculating successive transformations of coordinates, by pre-multiplying the transformation matrix between a frame and the previous one, it is possible to obtain the global transformation matrix of the arm, which obtains coordinates of the center of the probe sphere with respect to the base of the PCMA as

$$\begin{cases} {}^0T_6 = {}^0A_1 {}^1A_2 {}^2A_3 {}^3A_4 {}^4A_5 {}^5A_6, \\ \bar{X}_{\text{PCMA}} = {}^0T_6 \bar{X}_{\text{Probe}} \end{cases} \quad (4)$$

If small parameter errors occur in PCMA kinematic parameters $\theta_i, d_i, a_i, \alpha_i$ and β_i , the resultant error occurred in the homogenous transformation in Eq. (2) is given in Eq. (4) using Taylor expansion theory, assuming that the errors are small so the higher-order terms are negligible.

$$dA_i = \frac{\partial A_i}{\partial \theta_i} \Delta \theta_i + \frac{\partial A_i}{\partial d_i} \Delta d_i + \frac{\partial A_i}{\partial \alpha_i} \Delta \alpha_i + \frac{\partial A_i}{\partial \beta_i} \Delta \beta_i. \quad (5)$$

The final PCMA positional and orientation changes can be calculated through

$$\begin{aligned} dT_N &= \frac{\partial T_N}{\partial \theta_i} \Delta \theta_i + \frac{\partial T_N}{\partial d_i} \Delta d_i + \frac{\partial T_N}{\partial a_i} \Delta a_i \\ &+ \frac{\partial T_N}{\partial \alpha_i} \Delta \alpha_i + \frac{\partial T_N}{\partial \beta_i} \Delta \beta_i + \dots + \frac{\partial T_N}{\partial \theta_N} \Delta \theta_N \\ &+ \frac{\partial T_N}{\partial d_N} \Delta d_N + \frac{\partial T_N}{\partial a_N} \Delta a_N + \frac{\partial T_N}{\partial \alpha_N} \Delta \alpha_N + \frac{\partial T_N}{\partial \beta_N} \Delta \beta_N, \end{aligned} \quad (6)$$

$$\text{where, } \delta T = \begin{pmatrix} 1 & -\delta_z & \delta_y & \Delta_x \\ \delta_z & 1 & -\delta_x & \Delta_y \\ -\delta_y & \delta_x & 1 & \Delta_z \\ 0 & 0 & 0 & 1 \end{pmatrix}.$$

Equating the three positional components on the left and right sides of Eq. (7), we have

$$\Delta = \begin{pmatrix} \Delta_x \\ \Delta_y \\ \Delta_z \end{pmatrix} = M_\theta \Delta\theta + M_d \Delta d + M_\alpha \Delta\alpha + M_\beta \Delta\beta. \quad (7)$$

Equating the three differential rotational components on the right and left sides of Eq. (7), we have

$$\delta = \begin{pmatrix} \delta_x \\ \delta_y \\ \delta_z \end{pmatrix} = R_\theta \delta\theta + R_\alpha \delta\alpha + R_\beta \delta\beta. \quad (8)$$

By combining Eqs. (7) and (8), we can write the error model in matrix format as

$$\begin{pmatrix} \Delta \\ \delta \end{pmatrix} = \begin{pmatrix} M_\theta \\ R_\theta \end{pmatrix} \Delta\theta + \begin{pmatrix} M_d \\ 0 \end{pmatrix} \Delta d + \begin{pmatrix} M_\alpha \\ R_\alpha \end{pmatrix} \Delta\alpha + \begin{pmatrix} M_\beta \\ R_\beta \end{pmatrix} \Delta\beta, \quad (9)$$

where, $\Delta\theta = (\Delta\theta_1, \Delta\theta_2 \dots \Delta\theta_N)^T$, $\Delta d = (\Delta d_1, \Delta d_2 \dots \Delta d_N)^T$, $\Delta\alpha = (\Delta\alpha_1, \Delta\alpha_2 \dots \Delta\alpha_N)^T$, $\Delta\beta = (\Delta\beta_1, \Delta\beta_2 \dots \Delta\beta_N)^T$, M_θ , M_d , M_α , M_β , R_θ , R_α and R_β are constant coefficient matrices depending on PCMA's configuration.

In an alternative way, the relationship between differential position and orientation change with respect to the differential changes of kinematic parameter can be written as^[11,12]

$$\Delta X = J \cdot \Delta P, \quad (10)$$

where, $\Delta X = (\Delta x, \Delta y, \Delta z, \delta x, \delta y, \delta z)^T$ represents the end-effectors' position and orientation errors; $\Delta P = (\Delta\theta, \Delta d, \Delta\alpha, \Delta\beta)$ represents the PCMA kinematic parameter errors. J is identification Jacobian matrix as defined in Eq. (11):

$$J = \begin{pmatrix} M_\theta & M_d & M_\alpha & M_\beta \\ R_\theta & 0 & R_\alpha & R_\beta \end{pmatrix}. \quad (11)$$

After the PCMA kinematic model and parameters have been established, in order to know the influence of the temperature on the PCMA performance, it is crucial to identify the thermally-induced errors.

Internal heat sources and ambient heat sources result in arm temperature changes. The temperature variation not only causes link expansion but also structure distortions. In order to maintain the PCMA's accuracy, thermal errors must be estimated on-line during its operation. Therefore, a link between the error model and the physical parameters of the arm must be established in order to model the error with respect to changes in all arm geometric parameters. This link can

be obtained by relating variation in every parameter with the temperature changes by functions like the ones shown in

$$\begin{cases} \delta a_i = f_{a_i}(T) \\ \delta d_i = f_{d_i}(T) \\ \delta \alpha_i = f_{\alpha_i}(T) \\ \delta \theta_i = f_{\theta_i}(T) \\ \delta \bar{X}_{Probe} = f_{\bar{X}_{Probe}}(T) \end{cases}. \quad (12)$$

It is difficult to analytically describe the arm performance with thermal changing; the function shown in Eq. (12) is obtained from comprehensive data characterizing the behavior of the PCMA. Furthermore, every function will be modeled as ordinary polynomial covering the nominal working temperature range of the PCMA. An approximation by ordinary polynomial will be effective because expected temperature range is covered. It is not recommended to use a model extrapolating to temperature ranges out of the expected and measured one for the device in any case. The first step to obtain the functions in Eq. (12) is to find out the values of different geometrical parameters of the arm at different temperatures. As explained earlier, using the kinematic model of the PCMA, an optimization method can be developed in order to find the kinematic parameters that minimize the error induced by thermal changes. These parameters are needed at different temperatures to obtain the functions in Eq. (12) by applying regression techniques.

According to Eqs. (10) and (12), it is possible to model every kinematic parameter at different temperatures as shown in

$$P_i = P_i(T_{ref}) + \delta P_i, \quad (13)$$

where, $\delta P_i = f_i(T_i - T_{ref})$.

Thus, the vector P_i containing the parameters to be optimized is composed by increments in every parameter at different temperatures with respect to reference temperature.

With the values of geometrical parameters at different temperatures, it is possible to obtain the polynomials representing the relation between the variation in every parameter and the environmental temperature measured once the equipment is thermally stable. The first step of the approximation process is to decide the order of the polynomial. Owing to the regression method used, the limit for the order is the number of temperature values used, which are five in this case. The general approximation function for every parameter is given by

$$P_i(T) = P_i(T_{ref}) + C_{P_i} + \sum_{m=1}^n (A_{P_i,m} \cdot \Delta T^m), \quad (14)$$

where, $\Delta T = T - T_{ref}$ and with $P_i(T_{ref})$ representing the value of the parameter at reference temperature. C and A , respectively, represent the independent term and the

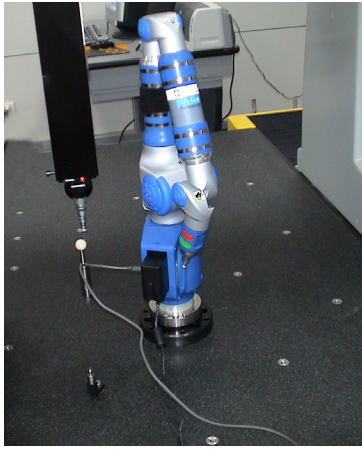


Fig. 2. The experimental layout.

coefficients of the ordinary polynomial modeling the increment of every parameter.

In order to choose the most adequate order for the polynomial, different alternatives were studied in the parameters. Finally, an order of four was chosen. Smaller residuals were obtained for order five polynomials, but the better fit of the measured points resulted in big variations between points, which implied inadequate corrections at intermediate points. Equation (15) can be written as

$$P_i(T) = P_i(T_{ref}) + C_{P_i} + A_{P_i1} \cdot \Delta T^1 + A_{P_i2} \cdot \Delta T^2 + A_{P_i3} \cdot \Delta T^3 + A_{P_i4} \cdot \Delta T^4. \quad (15)$$

After the thermally-induced error correction model is proposed, experimental studies are conducted to check validity of the theoretical results.

Figure 2 shows the experiment layout; the calibration artifacts are standard ball and beams, which can be placed at different positions on the working platform of CMM. The distance between standard ball and beam can be accurately determined by CMM with an accuracy of 0.1 μm . During the calibration, we used PCMA to

Table 1. Distance errors in d/mm

Temperature (°C)	After correction		Before correction	
	Maximum error	Median error	Maximum error	Median error
16	0.130	0.070	0.050	0.032
18	0.090	0.050	0.020	0.014
20	0.085	0.080	0.043	0.038
22	-0.070	-0.042	0.040	0.034
24	-0.100	-0.050	0.041	0.032
26	-0.080	-0.048	0.048	0.035
28	-0.110	-0.060	0.046	0.033
30	-0.150	-0.080	0.044	0.036

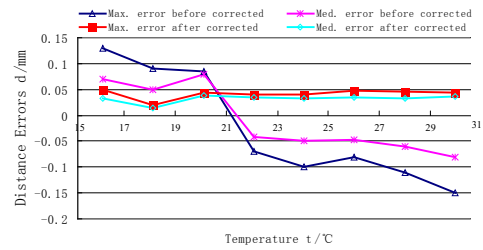


Fig. 3. Distance error of PCMA at different temperatures before and after correction.

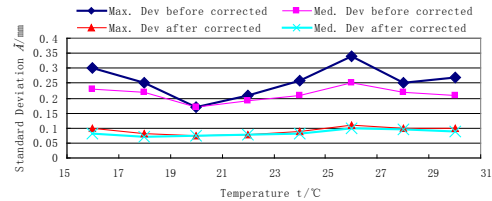


Fig. 4. Standard deviation of PCMA at different temperatures before and after correction.

measure the distance between standard ball and beam at different temperatures (16°, 18°, 20°, 22°, 24°, 26°, 28° and 30°C), and the correction model has been applied to these data in order to validate the performance after and before correction. The distance measured by the PCMA and CMM is compared. The experimental results are shown in Figs. 3 and 4.

As shown in Fig. 3, the deviations in PCMA distance error values with respect to the normal distance are calculated to evaluate the ability of the correction to reproduce the calibration conditions at considered temperatures. The distance error experimented results of before and after corrected, using thermally induced errors model are shown in Table 1.

As shown in Fig. 4, the standard deviation before and after correction is shown in Table 2.

Based on the above experiments, it is clearly concluded that the error results obtained by applying thermally-induced error model improved with respect to

Table 2. Standard deviation before and after correction

Temperature (°C)	After correction		Before correction	
	Maximum deviation	Median error	Maximum error	Median error
16	0.300	0.230	0.100	0.080
18	0.250	0.220	0.080	0.070
20	0.170	0.170	0.075	0.075
22	0.210	0.190	0.078	0.077
24	0.260	0.210	0.090	0.080
26	0.340	0.250	0.110	0.100
28	0.250	0.220	0.100	0.095
30	0.270	0.210	0.100	0.090

the non-corrected values. Once the temperature corrections are applied, the deviation of PCMA at different temperatures is in the range of $\pm 10 \mu\text{m}$. Although the results show a dramatic improvement with respect to the non-corrected values, it may be necessary to establish a more accurate method for approximation. Even an approximation to every parameter by temperature zones may be considered, because the temperature does not introduce any variation pattern detectable in the parameters.

A novel comprehensive thermally-induced error correction model is developed for PCMA. This model is able to correct the errors due to temperature changes, not only in the temperature used to calculate it but also in other validation intermediate temperatures. A general methodology is developed to calibrate these errors simultaneously. Based on this model, corresponding temperature variations, principle component analysis, the thermally-induced errors are corrected by measuring a standard artifact placed in several positions. The experimental results show that the accuracy obtained by applying thermally-induced error model improves with respect to the non-corrected values. Once the temperature corrections are applied, the deviation of PCMA at different temperatures is in the range of $\pm 10 \mu\text{m}$.

This study was supported by the National High Technology Research and Development Program (863

Program) of China (No. 2013AA06A411), the National Natural Science Foundation of China (No. 51304190), and the Natural Science Foundation of Jiangsu Province (no. BK2011226). The authors would like to express their sincere thanks to them.

References

1. S. Jorge, Y. J. Antonio, J. Roberto, and A. Juan-José, *Precis. Eng.* **33**, 476 (2009).
2. S. Jorge, A. Juan-José, Y. José-Antonio, and P. Jorge, *Precis. Eng.* **32**, 251 (2008).
3. K. Igor and F. Adolf, *Precis. Eng.* **25**, 90 (2001).
4. W. L. Liu and Z. K. Wang, *Meas. Sci. Technol.* **21**, 6 (2010).
5. J. O. Harris and A. D. Spence, *Int. J. Mach. Tool. Manuf. Precis. Eng.* **44**, 65 (2004).
6. X. Y. Wang, S. G. Liu, G. X. Zhang, B. Wang, and L. F. Guo, *Key Eng. Mater.* **381**, 161 (2008).
7. W. L. Liu and Z. K. Wang, *Meas. Sci. Technol.* **21**, 1 (2010).
8. J. H. Jung, J. P. Choi, and S. J. Lee, *J. Mater. Process. Technol.* **174**, 56 (2006).
9. G. Y. Zhang, T. X. Sun, L. Y. Wang, and X. P. Xu, *Chin. J. Mech. Eng.* **20**, 53 (2007).
10. J. P. Kruth, L. Zhou, C. Van den Bergh, and P. Vanherck, *Int. J. Adv. Manuf. Technol.* **21**, 874 (2003).
11. T. Ozel, *Int. J. Adv. Manuf. Technol.* **27**, 960 (2006).
12. S. W. Lin, P. P. Wang, Y. T. Fei, and C. K. Chen, *Int. J. Adv. Manuf. Technol.* **30**, 879 (2006).
13. S. Jamali, A. Kazemi, and H. Shateri, *Int. Rev. Electr. Eng.* **5**, 619 (2010).